Bol. Soc. Paran. Mat.
©SPM – E-ISSN-2175-1188
SPM: www.spm.uem.br/bspm

(3s.) **v. 2026 (44) 4** : 1–12.
ISSN-0037-8712
doi:10.5269/bspm.80383

Squeeze Film Behaviour Between Two Spheres: An Analysis Considering Pressure Dependent Viscosity and Couple-Stress Fluid Lubrication

Lakshmi R. [1], Hanumagowda B. N. [1,2], Siddharam Patil [3]

ABSTRACT: This paper aims to examine the collective influence of pressure-dependent viscosity in particular piezo viscous dependency (PDV) and couple stress fluid lubrication in a sphere-to-sphere configuration. Recognizing the limitations of the classical Reynolds equation, which neglects microstructural effects and assumes constant viscosity, this study derives a modified Reynolds equation incorporating both pressure-dependent viscosity and couple stress lubrication. The analysis yields a closed-form expressions for key bearing characteristics, including pressure, load-carrying capacity, and squeeze time. The findings indicate that increasing the values of radius ratio, couple stress, and piezo-viscous parameter leads to an increase in pressure and load-carrying capacity, and also results in a longer effective squeezing time. The escalating demand for high-precision and high-load-carrying capacity in modern machinery necessitates a deeper understanding of these factors to optimize system performance and prevent premature failure.

Key Words: Couple stress fluid, pressure dependent viscosity, squeeze film.

Contents

1. Introduction

Squeeze film lubrication is vital in numerous mechanical systems involving relative normal motion between surfaces, including biomechanical devices, joints, and bearings. Precise modelling of such systems is essential to figure out load capacity, layer thickness, and general stability of these systems. The dynamics of squeezing films are essential in numerous technical applications, such as braking systems lubricating systems, and biomechanics, especially when it comes to synovial joints [1] and [2]. Wu et.al. [3] focused at how squeeze film lubrication works between the slipper and swashplate of an axial piston pump. Key parameters like leakage flow, film thickness of slipper lubricant, pressure distribution of sealing land, and load carrying capacity are evaluated to assess the slipper oil film's performance. Conventional Newtonian fluid models often fall short in accurately predicting the performance of lubricants, especially when dealing with complex fluids like polymer-thickened oils or synovial fluids that exhibit non-Newtonian characteristics. To address these shortcomings, modeling of non-Newtonian lubricants like couple stress fluids has become essential. Stokes [4] first introduced the couple stress theory, which accounts for the microstructure of lubricants—particularly important in thin films or when using additives or polymer-based lubricants. Lin [5,6,7,8,9] and others [10,11,12,13,14] have significantly contributed to the understanding of lubrication problems by extending couple stress theory. Specifically, Lin investigated the rheological effects of couple stress in various bearing configurations: finite journal bearings [5] and [6], hemispherical bearings (relevant to synovial joints) [7], rotor bearings [8], and long partial journal bearings [9]. The studies [5] and [6] have consistently demonstrated that couple stresses have a notable impact on the dynamic and static lubrication characteristics of the bearings. Due to its comparative mathematical tractability, the couple stress fluid model has gained wide acceptance in lubrication research considering various geometries. Ramaniah . [10] investigated between finite plates, while Ramanaiah and Sarkar [11] explored thrust bearings. Bujurke and Jayaraman [12] focused on applications relevant to synovial joints,

2020 *Mathematics Subject Classification:* 76A05, 76D08, 76D99.
Submitted November 26, 2025. Published February 05, 2026

and Sinha and Singh considered cavitation effects in rolling contact bearings. Further contributions include Bujurke and Naduvinamani's [14] work on lightly loaded cylinders in combined rolling, sliding, and normal motion, and Ramaniah's [15] analysis of slider bearings. The presence of couple stresses in these models leads to enhancement of load-carrying capacity and an extension of the system's response time. Following the incorporation of couple stress effects, subsequent research [16,17,18,19,20,21] has broadened the scope to include additional factors such as magneto-hydrodynamic effects, slip velocity, pressure-dependent viscosity, surface roughness, and porosity, across various geometric configurations. For instance, Rajashekar and Kashinath [16] investigated the combined influence of surface roughness and magnetohydrodynamics in a configuration consisting of a sphere and a porous plane surface, whereas Naduvinamani et al. [17] between porous circular stepped plates while Salma and Hanumagowda [18] between porous curved annular plates. Additionally, Salma. et al., [19] examined surface roughness with couple stress fluid and magnetohydrodynamics on porous curved annular plates. These studies found that the combined influence of these factors generally increases pressure, load, and squeezing time whereas introducing porosity can decrease bearing characteristics but potentially improve bearing life. Vinutha et al. [20] and [21] further explored the effects of adding slip velocity, noting improvements in bearing characteristics. Traditional squeeze film analyses often relied on the assumption of constant-viscosity Newtonian fluids. However, it's now well-recognized that lubricant viscosity varies with pressure, particularly in the high-pressure conditions found in heavily loaded contacts. Overlooking this pressure-viscosity dependence can lead to inaccurate predictions of film thickness and performance degradation in practical systems. Pioneering work by Barus [22] explored the viscosity of fluids under varying pressures, and Gould [23] further advanced the understanding of pressure-dependent viscosity. More recently, numerous studies [24,25,26,27,28,29,30,31] have investigated combined effect of couplestress and pressure-dependent viscosity variations. Lin [24] examined the combined effect in wide parallel-plate configurations, while Hanumagowda et al., [25] studied the combined effect between circular stepped plates [25] and porous circular stepped plates [26]. Singh [27] focused on circular plates, and Vasanth et al. investigated porous circular plates [28] and porous annular plates [29]. These studies generally found that the combined effect couple stresses and pressure-dependent viscosity significantly increases pressure and load of the system. Dass et al., [30] explored the combined effect with slip velocity on finite journal bearings, considering slip on the journal, bearing, or both, and found that high piezo-viscosity and slip velocity enhance pressure and load. They also observed that the frictional parameter decreases with slip on the bearing. Byeon et al., [31] added MHD to the combination and analyzed the effect between rough flat and curved circular plates. Additionally, Suresha et al. [32] also incorporated MHD into the combination and found an enhancement in pressure and load. Sphere-to-sphere configurations are indeed relevant in various applications where curvilinear contact governs hydrodynamic behavior, including robotic grippers, joint mechanics, contact lenses, capillary bridge forces, microfluidics, precision instrument bearings, ball bearings, and gear contacts. Unlike simplified geometries like flat or cylindrical interfaces, spherical contacts offer a more realistic representation of many practical systems. Existing research, such as the work by Lin et al. [33], indicates that non-Newtonian couple stresses significantly influence squeeze film characteristics between two spheres, particularly at lower film heights and with larger couple-stress parameters and radius ratios. Recently Anjum et al. [34] have demonstrated that MHD effects can further enhance pressure generation and load-carrying capacity in these configurations due to stronger electromagnetic damping effects. Acknowledging the limited existing research on sphere-to-sphere configurations, this article introduces a novel approach to address this gap by investigating squeeze film couple stress lubrication between two spheres, explicitly considering pressure-dependent viscosity. This is motivated by the understanding that the interplay between pressure-dependent viscosity and couple stresses is crucial for optimizing system performance and preventing premature failure.

2. Mathematical Model of the Problem

The system under consideration is comprised of two spheres, S_1 and S_2, with respective radii R_1 and R_2 where $R_1, R_2 \gg x$, as depicted in Figure 1. Sphere S_2 approaches S_1 with a squeeze velocity $v = -\dfrac{\partial h}{\partial t}$, where h represents the time-dependent gap between the spheres. The intervening space between S_1 and S_2 is filled with a couple stress lubricant. A cylindrical coordinate system (r, θ, y) is

employed for analysis, with the origin positioned at the midpoint of the minimum film thickness, h_m. The upper and lower film thicknesses are denoted as h_2 and h_1, respectively, such that the total film thickness, given by Hamrock [35], is

$$h = h_1 + h_2,$$

where

$$h_1 = \frac{h_m}{2} + \frac{r^2}{2R_1}, \tag{1}$$

$$h_2 = \frac{h_m}{2} + \frac{r^2}{2R_2}, \tag{2}$$

and therefore

$$h = h_1 + h_2 = h_m + \frac{R_1 + R_2}{2R_1R_2} r^2.$$

The basic equation governing the flow is

$$\mu \frac{\partial^2 u}{\partial y^2} - \eta \frac{\partial^4 u}{\partial y^4} = \frac{\partial p}{\partial r}. \tag{3}$$

$$\frac{\partial p}{\partial y} = 0 \tag{4}$$

$$\frac{1}{r}\frac{\partial}{\partial r}(ru) + \frac{\partial v}{\partial y} = 0 \tag{5}$$

The relevant boundary conditions for velocity components are:

1. At the upper surface $y = h_2$

$$u = 0, \quad v = -\frac{\partial h}{\partial t}, \quad \frac{\partial^2 u}{\partial y^2} = 0 \tag{6.i}$$

2. At the lower surface $y = -h_1$

$$u = 0, \quad v = 0, \quad \frac{\partial^2 u}{\partial y^2} = 0 \tag{6.ii}$$

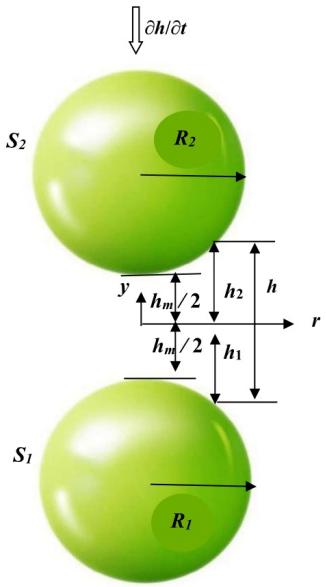

Figure 1: Effect of the velocity slip parameter h_0 and rotational parameter R_0 on velocity $f'(\eta)$

Solving equation (3) using the boundary conditions (6.i) and (6.ii), we get

$$u = \frac{1}{2\mu}\frac{\partial p}{\partial r}\left[\left(y^2 + (h_1 - h_2)y - h_1h_2 + 2l^2\right) - 2l^2\left(\frac{\cosh\left(\frac{2y + h_1 - h_2}{2l}\right)}{\cosh\left(\frac{h_1 + h_2}{2l}\right)}\right)\right] \tag{7}$$

Substituting equation (7) in (5) and integrating we get

$$\frac{1}{r}\frac{\partial}{\partial r}\left[\frac{r}{\mu}\frac{\partial p}{\partial r}\left(h^3 - 12l^2h + 24l^3\tan^{-1}\left(\frac{h}{2l}\right)\right)\right] = -12\frac{\partial h}{\partial t} \tag{8}$$

Pressure–dependent viscosity variation is given by

$$\mu = \mu_0 e^{\alpha p} \tag{9}$$

$$l = \left(\frac{\eta}{\mu}\right)^{1/2} = \left(\frac{\eta}{\mu_0 e^{\alpha p}}\right)^{1/2} = me^{-\alpha p/2}, \qquad m = \left(\frac{\eta}{\mu_0}\right)^{1/2}$$

$$\frac{\partial}{\partial r}\left[r\left(h^3e^{-\alpha p} - 12m^2he^{-2\alpha p} + 24m^3e^{-2.5\alpha p}\tanh\left(\frac{he^{\alpha p/2}}{2m}\right)\right)\frac{\partial p}{\partial r}\right] = 12r\mu_0\frac{\partial h}{\partial t}$$

$$\frac{\partial}{\partial r}\left[A(m,\alpha,h,p)\frac{\partial p}{\partial r}\right] = 12r\mu_0\frac{\partial h}{\partial t} \tag{10}$$

$$A(m,\alpha,h,p) = h^3e^{-\alpha p} - 12m^2he^{-2\alpha p} + 24m^3e^{-2.5\alpha p}\tanh\left(\frac{he^{\alpha p/2}}{2m}\right)$$

Using the following non dimensional quantities

$$r^* = \frac{r}{R_2}, \qquad h_1^* = \frac{h_m^*}{2} + \frac{r^{*2}}{2\alpha\beta}, \qquad h_2^* = \frac{h_m^*}{2} + \frac{r^{*2}}{2\beta}, \qquad h_m^* = \frac{h_m}{h_{m0}},$$

$$h^* = h_1^* + h_2^* = h_m^* + \frac{(\alpha+1)}{2\alpha\beta} r^{*2}, \qquad \alpha = \frac{R_1}{R_2}, \qquad \beta = \frac{h_{m0}}{R_2}, \qquad l^* = \frac{l}{h_{m0}}, \qquad p^* = \frac{p h_{m0}^2}{\mu R_2 \left(-\frac{\partial h}{\partial t}\right)}$$

$$\frac{1}{r^*}\frac{\partial}{\partial r^*}\left[A^*(G, h^*, l^*, p^*)\, r^* \frac{\partial p^*}{\partial r^*}\right] = \frac{12}{\beta} \tag{11}$$

$$A^*(G, h^*, l^*, p^*) = h^* e^{-Gp^*} - 12 l^{*2} h^* e^{-2Gp^*} + 24 e^{-2.5Gp^*} l^{*3} \tanh\left(e^{0.5Gp^*} \frac{h^*}{2l^*}\right)$$

$$\frac{\partial}{\partial r^*}\left\{\left[h^{*3} e^{-Gp^*} - 12 l^{*2} h^* e^{-2Gp^*} + 24 e^{-2.5Gp^*} l^{*3} \tanh\left(e^{0.5Gp^*} \frac{h^*}{2l^*}\right)\right] r^* \frac{\partial p^*}{\partial r^*}\right\} = \frac{12 r^*}{\beta}$$

$$\frac{\partial}{\partial r^*}\left\{\left[h^*(1 - Gp^*) - 12 h^* l^{*2}(1 - 2Gp^*) + 24 l^{*3}(1 - 2.5Gp^*) \tanh\left((1 + 0.5Gp^*)\frac{h^*}{2l^*}\right)\right] r^* \frac{\partial p^*}{\partial r^*}\right\} = \frac{12 r^*}{\beta} \tag{12}$$

Applying perturbation method

Put $p^* = p_0^* + G p_1^*$ in equation (12) and equating the coefficients of G^0 and G, we get

$$\frac{\partial}{\partial r^*}\left\{g_0^*(h^*, l^*)\, r^* \frac{\partial p_0^*}{\partial r^*}\right\} = \frac{12 r^*}{\beta} \tag{13}$$

$$g_0^*(h^*, l^*) = h^{*3} - 12 l^{*2} h^* e^{-2Gp^*} + 24 l^{*3} \tanh\left(\frac{h^*}{2l^*}\right)$$

$$\frac{\partial}{\partial r^*}\left\{g_0^*(h^*, l^*)\, r^* \frac{\partial p_1^*}{\partial r^*} + g_1^*(h^*, l^*)\, p_0^* r^* \frac{\partial p_0^*}{\partial r^*}\right\} = 0 \tag{14}$$

$$g_1^*(h^*, l^*) = -h^{*3} - 60 l^{*3} \tanh\left(\frac{h^*}{2l^*}\right) + 6 l^{*2} h^* \left(4 + \operatorname{sech}^2\left(\frac{h^*}{2l^*}\right)\right)$$

The pressure boundary conditions are

$$\frac{\partial p^*}{\partial r^*} = 0 \qquad \text{at } r^* = 0 \tag{15}$$

$$p^* = 0 \qquad \text{at } r^* = 1 \tag{16}$$

Integrating equation (13) and (14) using the pressure boundary conditions, we obtain

$$p_0^* = \frac{1}{\beta}\int_{r^*}^{1} \frac{6 r^*}{g_0^*(h^*, l^*)}\, dr^* \tag{17}$$

$$p_1^* = -\frac{6}{\beta^*}\int_{r^*}^{1} \left[\frac{g_1^*(h^*, l^*)}{\{g_0^*(h^*, l^*)\}^2}\, r^* p_0\right] dr^* \tag{18}$$

Hence the pressure distribution in the bearing is given by

$$p^* = \frac{6}{\beta^*}\left\{\int_{r^*}^{1} \frac{r^*}{g_0^*(h^*, l^*)}\, dr^*\right\} - G\frac{6}{\beta^*}\left[\int_{r^*}^{1} \left(\frac{g_1^*(h^*, l^*)}{\{g_0^*(h^*, l^*)\}^2}\, r^* p_0\right) dr^*\right] \tag{19}$$

The load carrying capacity is given by

$$W = 2\pi \int_0^{R_2} pr\, dr \tag{20}$$

Hence the load in non-dimensional form is

$$W^* = \frac{12\pi}{\beta^*}\left\{\left(\int_{r^*}^1 \frac{r^*}{g_0^*(h^*,l^*)}\, dr^*\right) r^* dr^*\right\} - G\frac{12\pi}{\beta^*}\left\{\left(\int_{r^*}^1 \left[\frac{g_1^*(h^*,l^*)}{\{g_0^*(h^*,l^*)\}^2}\, r^* p_0\right] dr^*\right) r^* dr^*\right\} \tag{21}$$

The squeeze film time is given by

$$T^* = \frac{W h_m^2 t}{\mu R_2^4} \tag{22}$$

$$T^* = \frac{12\pi}{\beta^*}\left\{\int_{h_f^*}^1 \left[\left(\int_{r^*}^1 \frac{r^*}{g_0^*(h^*,l^*)}\, dr^*\right) r^* dr^*\right] dh_m^*\right\} - G\frac{12\pi}{\beta^*}\left\{\int_{h_f^*}^1 \left[\left(\int_{r^*}^1 \left[\frac{g_1^*(h^*,l^*)}{\{g_0^*(h^*,l^*)\}^2} r^* p_0\right] dr^*\right) r^* dr^*\right] dh_m^*\right\} \tag{23}$$

3. Result and Discussion

The paper examines the combined effects of couple stress and piezo-viscous dependency from a theoretical standpoint on a sphere-to-sphere geometrical configuration. Employing Stokes micro-continuum theory and incorporating Baru's formula for piezo-viscous dependency, squeeze film characteristics have been analysed. The couple stress parameter ℓ^* varies from 0 to 0.4, the piezo-viscous parameter is taking values 0.0 and 0.4 and initial film radius parameter is taking a fixed value $\beta = 0.4$ throughout the study. The graphs show a comparison between piezo-viscous (solid line, $G = 0.04$) and iso-viscous cases (dotted line, $G = 0.0$).

Pressure

Fig.2 illustrates the effect of radius ratio parameter on fluid film pressure p^* against radial coordinate r^*. The analysis considers a couple stress fluid, maintaining a constant film thickness h_m^*. The results indicate that the presence of pressure-dependent viscosity leads to a higher fluid film pressure due to increased resistance to the flow. Furthermore, an increase in the radius ratio parameter also leads to an enhanced fluid film pressure. This can be stemmed as larger radius ratio indicates larger area of contact and a thinner fluid film, resulting in increased resistance to flow and consequently, an increased pressure within the lubricating film. This proposes that both pressure-dependent viscosity and the geometric configuration significantly affect the pressure distribution within the squeeze film. Fig. 3 exemplifies the impact of couple stress parameter l^* on the fluid film pressure profile p^* against radial coordinate r^* with a radius ratio $\alpha = 2$. The results indicate that including pressure-dependent viscosity and increasing the couple stress parameter leads to a significant increment in fluid film pressure. Physically, this indicates that the microstructure of the fluid, represented by the couple stress parameter l^*, provides additional resistance to flow, leading to higher pressures within the film. This effect is further intensified by the piezo-viscous dependency, as the resistance of fluid to flow increases further with increasing pressure.

Fig. 4 illustrates the plot of fluid film pressure p^* against r^*, by varying minimum film thickness h_m^*, by considering piezo-viscosity dependency ($G = 0.04$) and iso-viscous dependency ($G = 0.0$) in a couple stress fluid ($l^* = 0.3$). The results indicate that increasing the minimum film thickness leads to a decrease in fluid film pressure. This is because a larger film thickness provides a wider channel for the fluid to flow through, which reduces resistance to flow resulting in a lower pressure within the lubricating film. The effect is further enhanced by the pressure-dependent viscosity and couple stress within the fluid due to the lower pressure gradients.

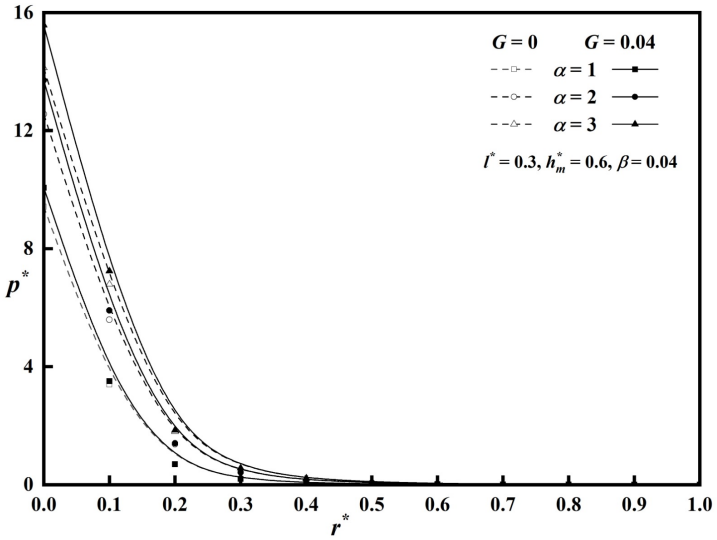

Figure 2: Relationship between dimensionless pressure p^* and radial co-ordinate r^* comparing piezo-viscous and iso-viscous cases, and by varying radius ratio α.

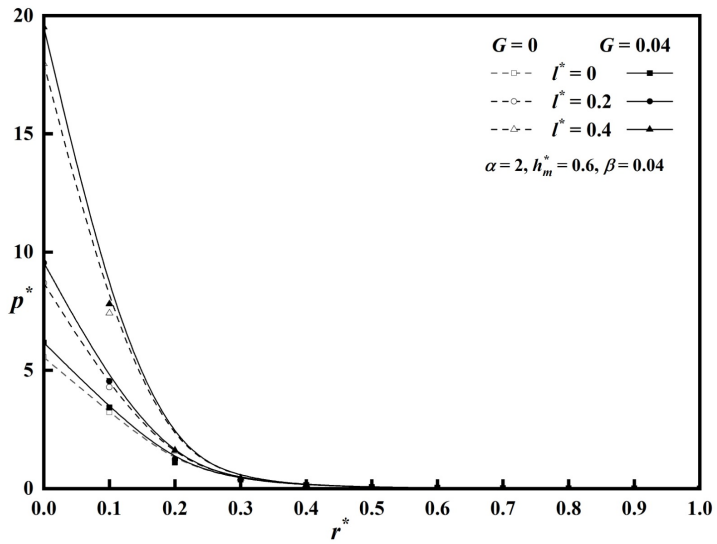

Figure 3: Relationship between dimensionless pressure p^* and radial co-ordinate r^* comparing piezo-viscous and iso-viscous cases, and by couple stress parameter l^*.

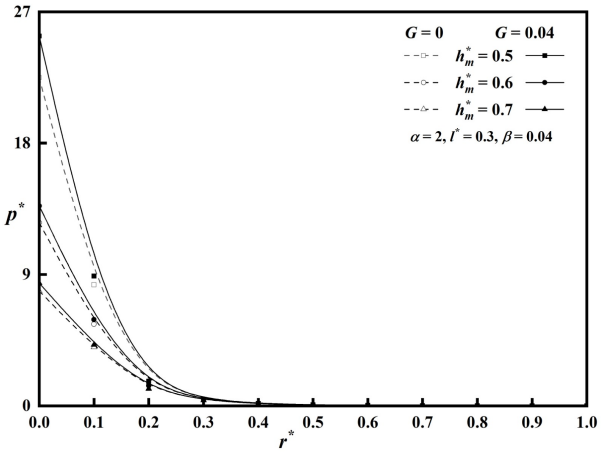

Figure 4: Relationship between dimensionless pressure p^* and radial co-ordinate r^* comparing piezo-viscous and iso-viscous cases, and by varying minimum film thickness.

Load Carrying Capacity

The relationship between the dimensionless load-carrying capacity W^* and film thickness h_m^* in the presence of a couple stress fluid l^* is depicted in Fig. 5. A comparative analysis is performed, contrasting the scenarios with and without pressure-dependent viscosity by varying radius ratio. It is observed that the load-carrying capacity increases with an increasing radius ratio parameter. Furthermore, this effect is amplified when pressure-dependent viscosity and couple stress fluid is considered. This can be attributed as increasing radius ratio increases contact area as well as volume of the fluid leading to an increase in load bearing capacity which in turn increases pressure and hence viscosity. This viscosity offers resistance to fluid flow. Moreover, couple stress also offers resistance to fluid flow thus enabling the film to have a larger load bearing capability.

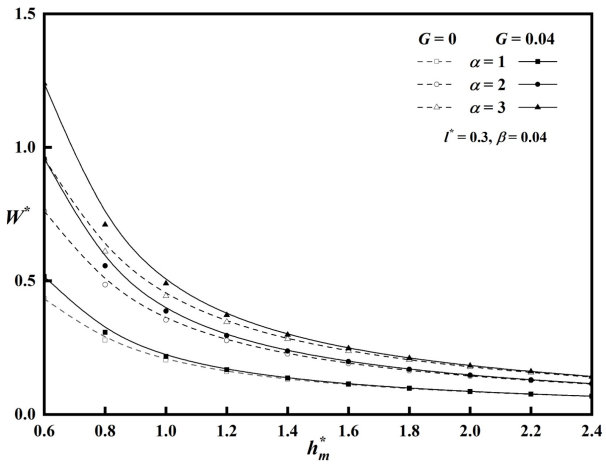

Figure 5: Relationship between dimensionless load W^* and minimum film thickness h_m^* by comparing piezo-viscous and iso-viscous cases, and by varying radius ratio parameter.

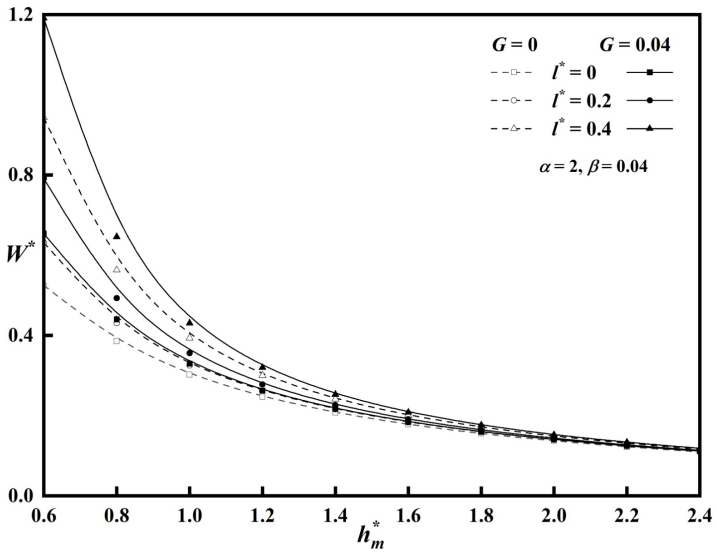

Figure 6: Relationship between dimensionless load W^* and minimum film thickness h_m^* by comparing piezo-viscous and iso-viscous cases, and by varying couple stress parameter.

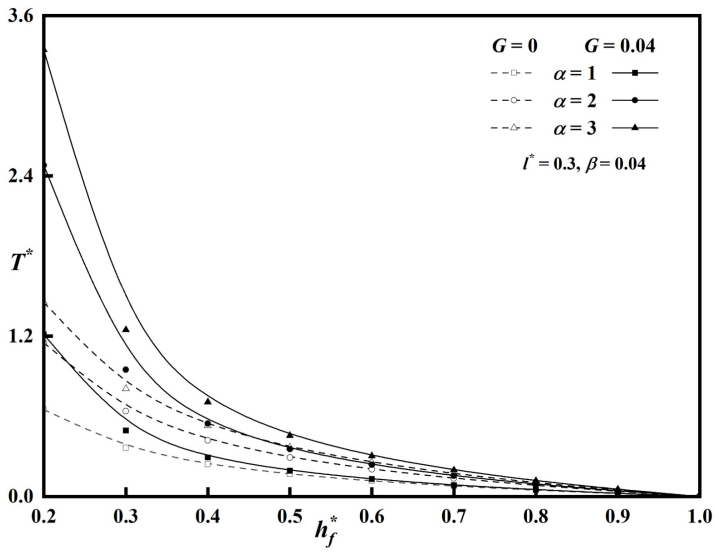

Figure 7: Relationship between squeezing time T^* and squeeze film height h_f^* by comparing piezo-viscous and iso-viscous cases, and by varying radius ratio parameter.

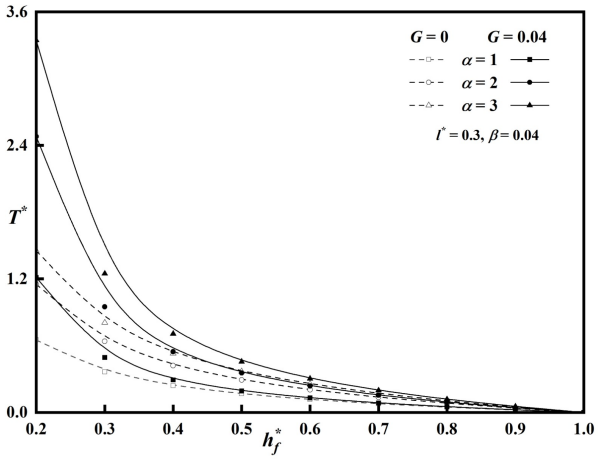

Figure 8: Relationship between squeezing time T^* and squeeze film height h_f^* by comparing piezo-viscous and iso-viscous cases and by varying couple stress parameter.

In Fig. 6 non-dimensional load W^* is plotted against film thickness h_m^* by varying l^* and considering piezo–viscous and iso-viscous cases, keeping radius ratio $\alpha = 2$ fixed. The findings show that an increase in the couple stress parameter enhances the load-carrying capacity of the squeeze film. The underlying reason is that a larger couple stress parameter implies stronger resistance to micro rotational motions in the fluid, effectively increasing the fluid's apparent viscosity thereby improves the film's ability to sustain higher loads. Moreover, in the presence of pressure-dependent viscosity, the increase in load results in elevated pressure, which further boosts the viscosity exponentially—intensifying the role of couple stress and indicating a synergistic effect between the two phenomena.Fig.7 illustrates the variation of squeezing time with respect to the squeeze film thickness h_f^*, considering scenarios with and without pressure-dependent viscosity and varying the radius ratio. The results indicate that squeezing time increases with an increasing radius ratio parameter. Physically, a larger radius ratio provides a greater surface area for the fluid to resist being squeezed out, thus prolonging the squeezing time. Moreover, at smaller gaps, the pressure increases significantly, leading to a substantial rise in viscosity when PDV is considered. Therefore, a higher squeezing time is observed in the presence of PDV, particularly at lower squeeze film thicknesses. Fig. 8 illustrates the relationship between squeezing time and squeeze film thickness h_f^* as the couple stress parameter is varied. The data reveals that squeezing time increases with an increasing couple stress parameter. Furthermore, the longest squeezing times are observed when pressure-dependent viscosity is considered, and these maximum squeezing times occur at lower squeeze film thicknesses. This can be attributed to the observation that as the film thickness decreases, the pressure within the film increases, causing the viscosity to rise exponentially. The increase in viscosity intensifies the influence of couple stress, which provides enhanced resistance to flow caused by internal micro-rotations and fluid interactions. This, in turn, leads to a notably extended squeezing time, particularly when the film thickness is small.

4. Conclusion

This research has examined how based on Baru's theory pressure-dependent viscosity, Stokes theory, couple stress effects, and the radius ratio influence the squeeze film behaviour between spherical surfaces. These effects are viewed through the key parameters G (PDV), l^* (couple stress) and α (radius ratio). By incorporating these parameters, the model provides a more precise depiction of lubricant performance under higher pressure conditions.

- The inclusion of couple stress—stemming from the fluid's internal microstructure—contributes to increased pressure load-bearing capacityand extends the squeeze film's response time.

- Increasing radius ratio significantly impacts the fluid film's volume and contact area, and thereby increases the film's capacity to increase the pressure and load bearing capability.
- Additionally, accounting for pressure-dependent viscosity, where viscosity rises sharply with pressure, enhances the efficacy of squeeze film characteristics.

Overall, the interaction between couple stress and pressure-dependent viscosity leads to more efficient squeeze film characteristics between two spheres, and is significant because it allows for the design of lubrication systems that can withstand higher loads and maintain a more stable film thickness under demanding conditions, particularly where precision and durability are essential—such as in advanced machinery and biomechanical applications like synovial joint modelling.

Acknowledgments

The authors would like to thank the referees for their valuable comments and suggestions, which helped improve the quality and clarity of this paper.

References

1. P.S. Walker, D. Dowson, M.D. Longfield, V. Wright, "Boosted lubrication in synovial joints by fluid entrapment and enrichment," *Annals of the Rheumatic Diseases*, **27**(6) (1968) 512–520.
2. J.S. Hou, V.C. Mow, W.M. Lai, M.H. Holmes, "An analysis of the squeeze-film lubrication mechanism for articular cartilage," *Journal of Biomechanics*, **25**(3) (1992) 247–259.
3. J.H. Wu, L.F. Ma, G. Cheng, A.H. Han, "Squeeze Film Effect and Its Influence on the Lubrication Characteristics of Slipper Oil Film under Pressure Pulse," *Shock and Vibration* (2023).
4. V.K. Stokes, "Couple stresses in fluids," *Physics of Fluids* **9** (1966) 1709–1715.
5. J. Lin, "Effects of couple stresses on the lubrication of finite journal bearings," *Wear*, **206**(1–2) (1997) 171–178.
6. J.R. Lin, "Squeeze film characteristics of finite journal bearings: couple stress fluid model," *Tribology International*, **31**(4) (1998) 201–207.
7. J.R. Lin, "Couple-stress effects on the squeeze film characteristics of hemispherical bearings with reference to synovial joints," *Applied Mechanical Engineering*, in press.
8. J.R. Lin, "Static characteristics of rotor bearing system lubricated with couple stress fluids," *Computers & Structures*, **62** (1997) 175–184.
9. J.R. Lin, "Squeeze film characteristics of long partial journal bearings lubricated with couple stress fluids," *Tribology International*, **30** (1997) 53–58.
10. G. Ramanaiah, P. Sarkar, "Squeeze films and thrust bearings lubricated by fluids with couple stress," *Wear*, **48** (1978) 309–316.
11. G. Ramanaiah, "Squeeze films between finite plates lubricated by fluids with couple stress," *Wear*, **54** (1979) 315–320.
12. N.M. Bujurke, G. Jayaraman, "The influence of couple stresses in squeeze films," *International Journal of Mechanical Sciences*, **24** (1982) 369–376.
13. P. Sinha, C. Singh, "Couple stresses in the lubrication of rolling contact bearings considering cavitation," *Wear*, **67** (1981) 85–91.
14. N.M. Bujurke, N.G. Naduvinamani, "The lubrication of lightly loaded cylinders in combined rolling, sliding and normal motion with couple stress fluid," *International Journal of Mechanical Sciences*, **32** (1990) 969–979.
15. G. Ramanaiah, "Slider bearings lubricated by fluids with couple stress," *Wear*, **52** (1979) 27–36.
16. M. Rajashekar, B. Kashinath, "Effect of Surface Roughness on MHD Couple Stress Squeeze-Film Characteristics between a Sphere and a Porous Plane Surface," *Advances in Tribology* (2012).
17. N.B. Naduvinamani, B.N. Hanumagowda, S.T. Fathima, "Combined effects of MHD and surface roughness on couple-stress squeeze film lubrication between porous circular stepped plates," *Tribology International*, **56** (2012) 19–29.
18. S.A. Baksh, H.B. Naganagowda, "Study of surface roughness with MHD and couple stress fluid on porous curved annular plates," *Tribology*, **62**(6) (2022) 12–31.
19. A. Salma, B.N. Hanumagowda, C.K. Sreekala, M. Taseer, "Couple-stress fluid flow through porous medium between curved circular and rough flat plates," *Chinese Journal of Physics*, **88** (2024) 991–1009.
20. R. Vinutha, B.N. Hanumagowda, K.R. Vasanth, "Effect of MHD, couple stress and slip on squeeze film lubrication of long cylinder and rough plate," *Tribology International*, **191** (2024) 109164.

21. R. Vinutha, B.N. Hanumagowda, K.R. Vasanth, G.K. Kumar, "MHD, couple stress and slip effects on squeeze film lubrication of rough triangular plates," *International Journal of Thermofluids*, **24** (2024) 100882.

22. C. Barus, "Isothermals, isopiestics and isometrics relative to viscosity," *American Journal of Science*, **45**(266) (1893) 87–96.

23. P. Gould, "High pressure spherical squeeze films," *Journal of Lubrication Technology*, **93**(1) (1971) 207–208.

24. J.R. Lin, L.M. Chu, W.L. Li, R.F. Lu, "Piezo-viscous dependency and non-Newtonian couple stresses in parallel-plate squeeze films," *Tribology International*, **44**(12) (2011) 1598–1602.

25. B.N. Hanumagowda, "Pressure-dependent viscosity and couple stress in squeeze-film lubrication between circular step plates," *J. Eng. Tribology*, (2015).

26. B.N. Hanumagowda, B.T. Raju, J. Santhosh Kumar, K.R. Vasanth, "Pressure dependent viscosity on couple stress squeeze film lubrication between porous stepped plates," *Journal of Physics: Conference Series*, **1000** (2018) 012081.

27. U.P. Singh, "Piezo-viscosity and couple stress effects on squeeze film between circular plates," *International Journal of Fluid Mechanics Research*, **41**(4) (2015) 368–378.

28. V.K.R. Rajendrappa, H.B. Naganagowda, J.S. Kumar, R.B. Thimmaiah, "Piezo-viscous and couple-stress effects in porous squeeze-film circular plates," *Journal of Advanced Research in Fluid Mechanics and Thermal Sciences*, **51**(2) (2018) 158–168.

29. K.R. Vasanth, B.N. Hanumagowda, S. Kumar, "Piezo-viscous and couple stress effects on squeeze-film porous annular plate," *Journal of Physics: Conference Series*, (2018).

30. T. Dass, S.R. Gunakala, D.M.G. Comissiong, "Couple stresses, variable viscosity and slip in finite journal bearings," *Ain Shams Engineering Journal*, **11**(2) (2020) 501–518.

31. H. Byeon et al., "MHD and viscosity variation in couple stress squeeze film lubrication between rough and curved plates," *Scientific Reports*, **13** (2023) 22960.

32. R. Suresha et al., "MHD, couple stress and viscosity variation on squeeze film characteristics of cylinder and rough plate," *SN Applied Sciences*, **5** (2023) 350.

33. J.R. Lin, L.M. Chu, W.L. Liaw, L.J. Mou, "Effects of non-Newtonian couple stresses on squeeze film characteristics between two spheres," *Proc. IMechE Part J*, **222** (2008) 693-701.

34. J. Anjum et al., "Squeeze film lubrication between two different spheres: MHD-couple stress model," *Tribology International*, **166** (2025) 109133.

35. B.J. Hamrock, *Fundamentals of Fluid Film Lubrication*, McGraw-Hill, New York, 1994.

Department of Mathematics,
School of Applied Sciences, REVA University,
India.
E-mail address: lakshmichabanurkar97@gmail.com

and

Department of Mathematics,
GM University, Davangere-577006
India.
E-mail address: hanumagowda123@rediffmail.com

and

Department of Science,
Government Polytechnic, Shorapur-585224,
India.
E-mail address: sidram100@gmail.com